Available online at www.sciencedirect.com
ScienceDirect
Journal of Solid State Chemistry 181 (2008) 777–782
JOURNAL OF SOLID STATE CHEMISTRY
www.elsevier.com/locate/jssc

Structural aspects of fast copper mobility in Cu_6PS_5Cl—The best solid electrolyte from Cu_6PS_5X series

A. Gagor[a,*], A. Pietraszko[a], D. Kaynts[b]

[a] *W. Trzebiatowski Institute of Low Temperature and Structure Research, PAS, P.O. Box 1410, 50-950 Wroclaw, Poland*
[b] *Uzhhorod State University, 46 Pidhirna St., Uzhhorod 294000, Ukraine*

Received 4 December 2007; received in revised form 9 January 2008; accepted 13 January 2008
Available online 26 January 2008

Abstract

The structural origin of fast copper conduction in Cu_6PS_5Cl single crystals is discussed. Cu_6PS_5Cl crystallises in the same cubic $F\bar{4}3m$ symmetry as the other Cu_6PS_5X's, $X = Cl, I, Br$. However, this phase is stabilised at much lower temperatures (down to 160 K) and is characterised by higher level of disorder in copper substructure. Complex domain structure developing at low temperatures proves that Cu_6PS_5Cl undergoes ferroelastic phase transition (PT) associated with cubic $F\bar{4}3m$ to monoclinic Cc symmetry change. The structural distortion connected with this transformation is very subtle. X-ray diffraction measurements show strong precursor phenomena below 205 K which correspond to the low temperature phase and point out to copper ordering in nano- or microscopic scale above the temperature of ferroelastic phase transition (PT). The pseudopotential based on copper joint probability density function is calculated along diffusion paths at 175 and 435 K.

Keywords: Argyrodites; Ionic conductors; Battery materials; Phase transitions

1. Introduction

Cu_6PS_5Cl crystals of the argyrodite family possess the best conduction properties among all Cu_6PS_5X solid electrolytes. At room temperature total conductivity is almost purely ionic and σ_t reaches $4.7 \times 10^{-4}\,S\,cm^{-1}$ [1,2]. Above 573 K character of conductivity changes to mixed ionic and electronic with equal contribution of these two components. Cu_6PS_5Cl reveals high copper conduction at both high and low temperatures. Beeken et al. showed that in the wide temperature range (from 170 to 480 K) conductivity of Cu_6PS_5Cl obeys Arrhenius law with activation energy of 0.29 eV without any indications of phase transitions (PTs) while the other family members, such as Cu_6PS_5I and Cu_6PS_5Br, undergo structural PTs in this temperature range, which suppress ionic conduction. Namely, Cu_6PS_5Br exhibits ferroelastic PT with symmetry change from $F\bar{4}3m$ to Cc at $T_c = (268 \pm 2)$ K and isostructural, superionic transformation at $T_s = 169$ K. Whereas Cu_6PS_5I pure crystals display two structural PTs, the first one at $T_1 = 274$ K with a change of symmetry to $F\bar{4}3c$ cubic superstructure and next one—ferroelastic—at $T_c = (143-169)$ K, connected with symmetry change from $F\bar{4}3c$ to Cc [3–5].

All PTs mentioned above are connected with the ordering of copper substructure and thus determine conditions for fast ion conduction. In the cubic $F\bar{4}3m$ phase copper ions are distributed statistically over many tetrahedral, triangular and linear coordination sites in the argyrodite-type framework $[PS_5X]$. In $F\bar{4}3c$ superstructure an ordering process of copper sublattice takes place. Finally, Cc phase is characterised by fully occupied copper sites. As a result, the ionic conductivity in Cu_6PS_5Br crystals is lower and activation energy is higher than in Cu_6PS_5I.

As regards Cu_6PS_5Cl compounds, it is reported that at room temperature they possess $F\bar{4}3m$ symmetry, common to all Cu_6PS_5X [1]. Although Cu_6PS_5Cl argyrodite was synthesised in the early seventies and characterised by different research groups, there is still lack of data regarding low temperature structures and polymorphic

*Corresponding author. Fax: +48 71 343 10 29.
E-mail address: a.gagor@int.pan.wroc.pl (A. Gagor).

0022-4596/$ - see front matter © 2008 Elsevier Inc. All rights reserved.
doi:10.1016/j.jssc.2008.01.026

PTs. Furthermore, similarly to Cu_6PS_5I, samples from different sources show a surprising diversity of thermodynamic and conduction properties. For example, specific heat measurements show two thermally induced second-order PTs at $T_1 = 241\,K$ and $T_2 = 165\,K$, whereas calorimetric data reveals first-order PT at $T = 235\,K$ [6,7].

In order to establish structural conditions supporting the best copper conduction in this compound in the group of Cu_6PS_5X argyrodites, we undertook X-ray single crystal study and domain structure observations. A combination of these two experimental methods allowed us to establish the temperature of superionic and ferroelastic PT as well as distribution of copper ions in the crystal. Additionally, on the basis of copper joint probability density function (PDF) we analysed the change of the pseudopotential along diffusion paths versus temperature.

2. Experimental details

The Cu_6PS_5Cl single crystals were obtained by the conventional vapour transport method (for more details see [8]). Optical microscopy observations were performed under the polarising microscope. For these studies samples were cut out from an as-grown crystal in the (001) crystallographic direction. The thickness of plates was about 0.15 mm. The thermal cycle applied to the samples was performed as follows: the sample was cooled down directly from room temperature to a temperature below T_c and then heated. The cooling and heating rate was 1 deg/min. The sample was held in Linkam cooling–heating stage and the temperature of the specimen was controlled within 0.1 K. The pictures were taken by a commercial digital camera.

Single crystal X-ray study was performed on a Kuma KM4CCD diffractometer with graphite-monochromated Mo $K\alpha$ radiation. For all samples numerical absorption correction was applied. The Crys. Allis. software version 1.170.32 (Oxford Diffraction) was used for the data processing and reciprocal space reconstruction. The structure model of isostructural Cu_6PS_5I crystal was applied [4] and refined by the full-matrix least-squares method using Jana2000 program package [9]. In order to account for the diffused electron density of copper, we extended the refinement on the anharmonic Gram–Chalier model of displacement parameters [10,11]. The displacement factors of Cu2 atoms at 295 and 435 K were refined in the third-order anharmonic approximation. The values of tensor C_{ijk} parameters are presented in supplementary materials in Table A.1. On the basis of copper joint PDF we analysed the change of the pseudopotential along diffusion paths versus temperature. In the case of resolved positions the potential difference between symmetrically inequivalent sites is given by [12]

$$V(\mathbf{x}_1) - V(\mathbf{x}_2) = -kT \ln[w_1 \mathrm{PDF}_1(\mathbf{x}_1)/w_2 \mathrm{PDF}_2(\mathbf{x}_2)]. \quad (1)$$

The diffraction data were collected within the 120–435 K range. Low temperature was maintained by a nitrogen-gas-flow cooling system (Oxford Cryosystem Controller), $\Delta = 0.3\,K$. The details of the crystal structure investigations at 175, 295 and 435 K can be obtained from the Fachinformationszentrum Karlsruhe, 76344 Eggenstein-Leopoldshafen, Germany (fax: +497247808666; e-mail: crysdata@fiz.karlsruhe.de) on quoting the depositary numbers CSD 418657 (175 K), 418658 (435 K) and 418659 (295 K). Lattice parameters were determined by Bond procedure [13] on a Bond diffractometer using a graphite monochromated Cu $K\alpha$ radiation. The accuracy of determination of lattice parameters $\Delta a/a$ was 1×10^{-4}.

3. Results and discussion

3.1. Domain structure and ferroelastic PT

Domain structure in Cu_6PS_5Cl crystals appears as a result of ferroelastic PT to monoclinic *Cc* phase. Photographs of domain structure of Cu_6PS_5Cl taken at 207, 189 and 176 K are shown in Figs. 1(a, b), (c), (d), respectively. Ferroelastic domains appear at 207 K around defects located near the edges of the plate. Fig. 1(b) presents an enlarged part of the sample with characteristic for monoclinic *Cc* phase orientation of domain walls [14]. On further cooling, the domain structure spreads to other areas of the sample. However, even at 176 K there are still some regions optically isotropic with cubic symmetry (dark areas of the sample).

Characteristic arrangement of those two phases in the sample at low temperature may indicate that the distribution of copper ions is not homogeneous as far as the ordering processes in copper substructure answers for the temperature of ferroelastic PT. Similarly to Cu_6PS_5I, the temperature of ferroelastic PT is very sensitive to copper distribution in the crystal. This problem has been widely discussed in the papers by Studenyak et al. [8,15]. Thus, the observed different temperatures of ferroelastic PT in Cu_6PS_5Cl are coupled with a deviation from copper stoichiometry and poor homogeneity of the samples. Moreover, superionic PT is related to ferroelastic PT with $T_s = T_c$, which is also observed in Cu_6PS_5I.

3.2. Precursor effects near the ferroelsatic PT

Reciprocal space reconstructions taken in the cubic $F\bar{4}3m$ phase at $T = 205\,K$ reveal additional, very weak and fuzzy diffraction peaks on $hk0.5$ type layers. We believe that those effects arise from monoclinic ordering of copper in nano- or microscopic scale above the temperature of ferroelastic PT, since the distribution of those reflections is characteristic for the monoclinic low temperature *Cc* phase. Fig. 2(a) shows the precursor effects at 205 K and Fig. 2(b) presents the same reciprocal space reconstruction taken in monoclinic phase at $T = 120\,K$. All diffraction peaks presented in this picture can be attributed to one of the 12 ferroelastic domains, which may appear in $\bar{4}3mFm$ transition [16].

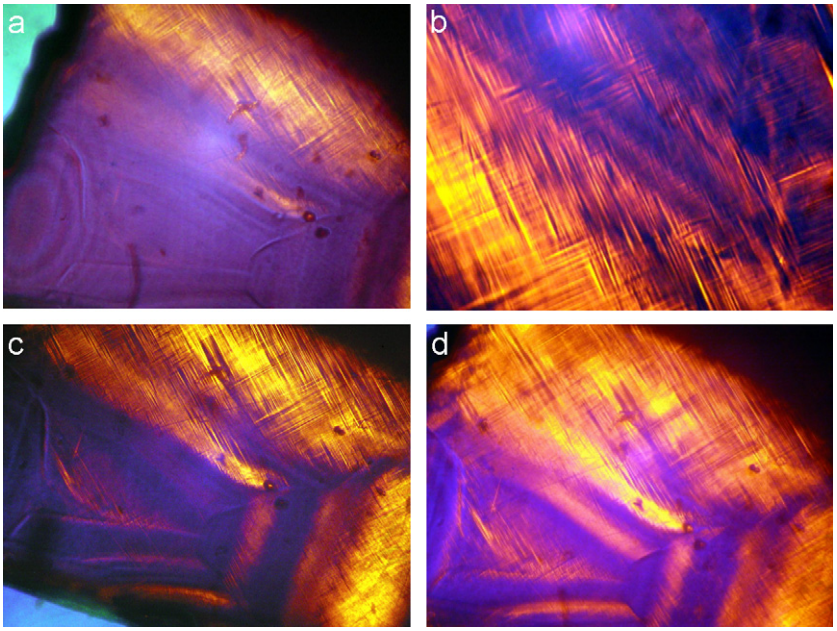

Fig. 1. Domain structure in Cu_6PS_5Cl: (a) $T = 207\,K$, (b) an enlarged part of the sample, $T = 207\,K$, (c) $T = 189\,K$, (d) $T = 176\,K$.

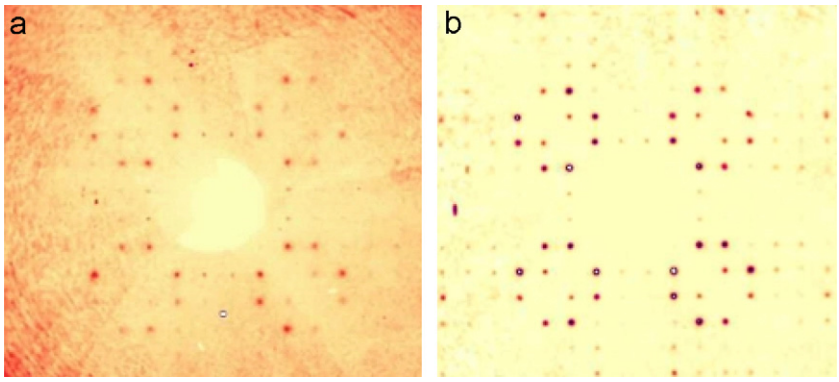

Fig. 2. Reciprocal space reconstruction of Cu_6PS_5Cl, $hk0.5$ layer, (a) regular $F\bar{4}3m$ phase, the precursor effects are well pronounced, $T = 205\,K$, (b) monoclinic phase, all observed diffraction peaks can be attributed to monoclinic domains, $T = 120\,K$.

Taking into account the results of ferroelastic domain observations, we can ascribe observed additional diffraction effects to copper ordering on crystal defects or connect them with the presence of small regions with higher copper concentration that spread the transition up. As the domain structure spreads to other areas of the crystal, with temperature decrease, the intensity of additional peaks increases. Then, below the temperature of PT, it rises rapidly, see Fig. A.1.

Similar phenomena were observed in Cu_6PS_5I above T_1, the temperature of structural PT from $F\bar{4}3m$ to $F\bar{4}3c$ phase [17]. Although both cubic $F\bar{4}3c$ and monoclinic phase are connected with ordering of copper substructure (in the former one the ordering process of copper is initiated and results in fully ordered copper positions in the latter one), we do not observe $F\bar{4}3c$ phase in Cu_6PS_5Cl crystals. This cubic superstructure gives additional diffraction peaks at $hk0$ layers, which were not observed in the case of Cu_6PS_5Cl.

The evolution of lattice parameters with temperature is presented in Fig. 3. Although the monoclinic distortion observed below 160 K is very small (lattice distortion at 135 K is of 0.005 Å), the characteristic domain structure, which appears below this temperature, evidence the monoclinic Cc symmetry (after Ref. [14]). Lattice parameters calculated in monoclinic system are as follows: $a = 11.829(9)$ Å, $b = 6.838(6)$ Å, $c = 11.831(7)$ Å, $\beta = 109.34(6)^\circ$ at 120 K. In the whole temperature range the volume of unit cell changes linearly and does not display any anomaly in the transition point. Such a small lattice deformation may indicate that the enthalpy of transition is also very small. This can further support our assumptions about the origin of precursors effects observed below 205 K.

3.3. Copper mobility in the cubic phase

The crystal structure of Cu_6PS_5Cl was determined at 175, 295 and 435 K. The crystallographic details are

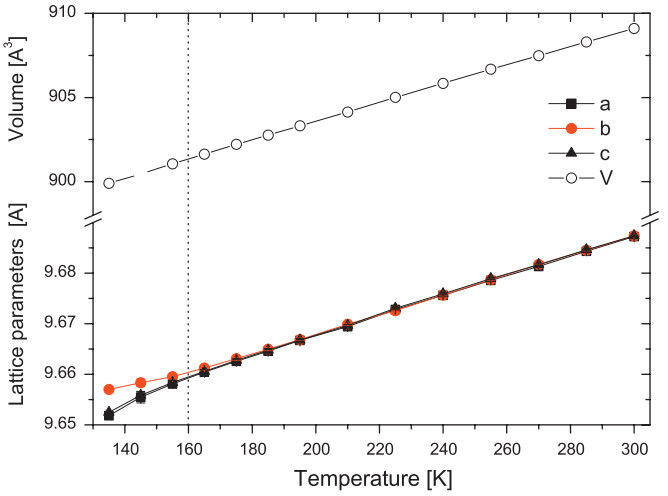

Fig. 3. Temperature dependence of unit cell parameters and volume of Cu_6PS_5Cl.

summarised in Table 1. The structure of low temperature phase was not determined because of the complex domain structure which appears below the PT and complicates much the diffraction data.

At the whole measured temperature range sample is in cubic $F\bar{4}3m$ phase, which is characteristic for high temperature argyrodite form [4,18]. At 175 K the rigid anion framework, which is built on $[PS_5I]$, accommodates 24 copper ions among 88 available positions in a unit cell. Copper ions are distributed statistically over three crystallographically independent sites: 16*e*, 24*g* and 48*h*. The details of the structure of Cu_6PS_5Cl at 175 K are presented in Table 2. The 16-fold Cu3 position is linearly coordinated by Cl and S atoms, the 24-fold Cu1 position is triangularly coordinated by three S atoms while 48-fold Cu2 position is coordinated tetrahedrally by three S and one Cl atom. The last two environments are slightly deformed because copper positions are shifted from the centre of triangle and tetrahedron towards S and the face of the tetrahedron, respectively.

Even at relatively low temperature (175 K) the copper positions are very close to each other in a unit cell with distances Cu1–Cu2 of 0.963(2) Å, Cu2–Cu3 of 1.280(13) Å, Cu2–Cu2′ of 2.204(3) Å. The distances do not have physical meaning although the positions form possible paths for copper migration in the structure. It was demonstrated that two-, three- and four-fold coordinated copper sites are separated by low energy barriers in solid halides and chalcogenides [19]. Thus, taking into account the close vicinity of these positions it is probable that the jumps of copper ions between them are easily thermally activated. The distribution of copper in a unit cell, which is present at 175 K in Cu_6PS_5Cl, is also observed in Cu_6PS_5I; however, in the latter compound copper accommodates Cu3 lattice site unless the temperature reaches 500 K. This may explain better conductivity of Cu_6PS_5Cl crystals.

Above the room temperature copper ions from Cu3 site shift from ideal linear coordination toward a new 48*h* position with deformed linear configuration with distances Cu3–Cl of 2.13 Å and Cu3–S of 2.29(4) Å. Similar process is also observed in selenium compound Cu_6PSe_5I above 500 K [17,20]. It confirms low stability of copper in low symmetry linear coordination [19]. The atomic parameters for copper with occupancy factors at 295 and 435 K are presented in supplementary materials in Table A.2. With temperature increase the distances Cu2–Cu3, Cu2–Cu2′ and Cu2–Cu1 shorten (see Fig. 4). Remarkable changes are observed for Cu2–Cu3 distance. Simultaneously, the values of copper displacement parameters increase. Consequently, it leads to the superposition of copper PDFs and reduction of potential barriers between copper positions. Fig. 5 presents coordination of copper ions and joint PDF of copper in Cu_6PS_5Cl at (a) 175 and (b) 435 K. The possible migration path for copper is presented in Fig. 5(a). The pseudopotential along Cu3–Cu2–Cu1 diffusion path has been calculated on the basis of joint PDFs, Fig. 5(c).

Analysis of the site potential for copper cations shows that the Cu1 has lower potential than Cu2 and its PDF is more contracted at all temperatures. With the temperature increase the potential barrier between Cu1 and Cu2 lowers slightly from 0.07 eV at 175 K down to 0.05 eV at 435 K,

Table 1
Experimental details

Nominal composition	Cu_6PS_5Cl		
Temperature (K)	175	295	435
Wavelength (Å)	Mo $K\alpha$/0.71069		
Crystal system, space group	Cubic, $F\bar{4}3m$		
Z, Pearson's code	4, cF52		
Lattice parameters (Å)	9.668(1)	9.688(1)	9.695(1)
Volume (Å^3)	903.8(2)	909.3(2)	911.2(2)
Calculated density (g/cm^3)	4.57	4.57	4.47
2θ range (deg)	56.2	92.5	92.4
Reflections collected/unique	2148/141	4299/446	4336/448
R_{int}	0.044	0.051	0.052
Data/parameters	141/20	446/23	448/27
Goodness of fit	1.4	1.4	1.4
R_1, wR_2 [$I>3\sigma(I)$]	0.021, 0.032	0.037, 0.043	0.040, 0.046
R_1, wR_2 (all data)	0.022, 0.033	0.040, 0.044	0.048, 0.049
Extinction coefficient	0.010(6)	0.040(3)	0.040(6)

Table 2
Wyckoff positions (W), site symmetry (S), fractional atomic coordinates, isotropic displacement parameters and site occupation factors for Cu_6PS_5Cl ($F\bar{4}3m$, $T = 175$ K)

Atom	W	S	x	y	z	U_{iso}	Sof.
Cl	4*a*	$\bar{4}3m$	0	0	0	0.0247(4)	1
P	4*b*	$\bar{4}3m$	0	0	0.5	0.0068(3)	1
S1	4*d*	$\bar{4}3m$	0.25	0.25	0.75	0.0178(3)	1
S2	16*e*	.3*m*	0.3774(1)	0.3774(1)	0.3774(1)	0.0103(2)	1
Cu1	24*g*	2.*mm*	0.25	0.25	0.9750(1)	0.0261(3)	0.574(3)
Cu2	48*h*	..*m*	0.1797(2)	0.3203(2)	0.5185(2)	0.0255(6)	0.224(3)
Cu3	16*e*	.3*m*	0.1177(13)	0.1177(13)	0.1177(13)	0.0033(5)	0.022(2)

which is characteristic for Cu_6PS_5X. Copper ions move almost without restraints along the edge of $S(Cl)_4$ tetrahedra. A significant decrease of the potential barrier is observed between Cu3 and Cu2 which implies an important role of Cu3 position in copper migration process. The height of this barrier ($\Delta E = 0.135$ eV at 435 K) determines the highest potential barrier among the pseudocluster of copper (see Fig. 6), which is concentrated on one $S(Cl)_4$ tetrahedron. Its value is comparable with the activation energy determined from conductivity measurements ($\Delta E = 0.22$ eV [1], $\Delta E = 0.29$ eV [2]) even though, it only contains information about the hopping barrier within tetrahedral cluster. Consequently, the real potential barrier is higher.

Contrary to Cu_6PS_5I we observe a connection of copper clusters via additional copper position at high temperature. At 435 K difference Fourier map shows new maximum (Cu4) at 16*e* position (see Fig. 6). It is tetrahedrally coordinated by one chlorine and three sulphur ions with distances Cu4–Cl of 2.183(1) Å, Cu4–S2 of 2.407(1) Å and with the distance of 1.564(6) Å to the nearest copper Cu2. Unfortunately, the weak electron density of this position disqualified it from the refinement. Thus, we were not able to calculate the joint PDF of Cu4. It is probable that appearance of copper at this position is related with diffusion of chlorine ions from the structure. This process takes place at high temperatures and as a consequence produces 12% of vacancies at chlorine sites. Simultaneously, the redox processes lead to reduction of copper ions to metallic copper, which results in increase of electronic contribution to the total conductivity of Cu_6PS_5Cl and mixed ionic–electronic character of conductivity at high temperatures. Moreover, the metallic tint of the sample at 435 K corroborates the reduction of copper ions.

Taking account of problems discussed above the possible conduction paths between neighbouring copper clusters have been calculated on the grounds of the nearest Cu2

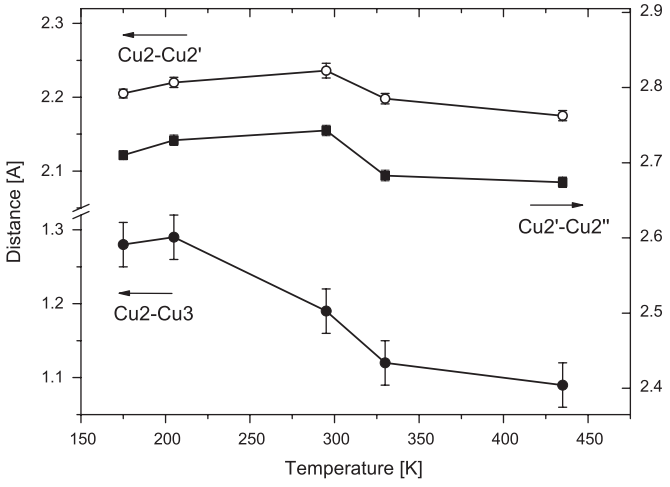

Fig. 4. The change of the distances between copper inside one copper cluster (Cu2–Cu2′ and Cu2–Cu3) and between two neighbouring clusters (Cu2′–Cu2″) versus temperature in Cu_6PS_5Cl.

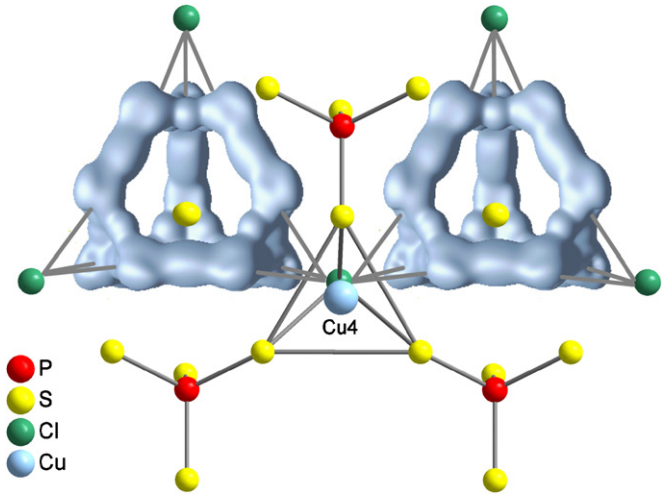

Fig. 6. Copper clusters and coordination of copper Cu4 in Cu_6PS_5Cl, $T = 435$ K.

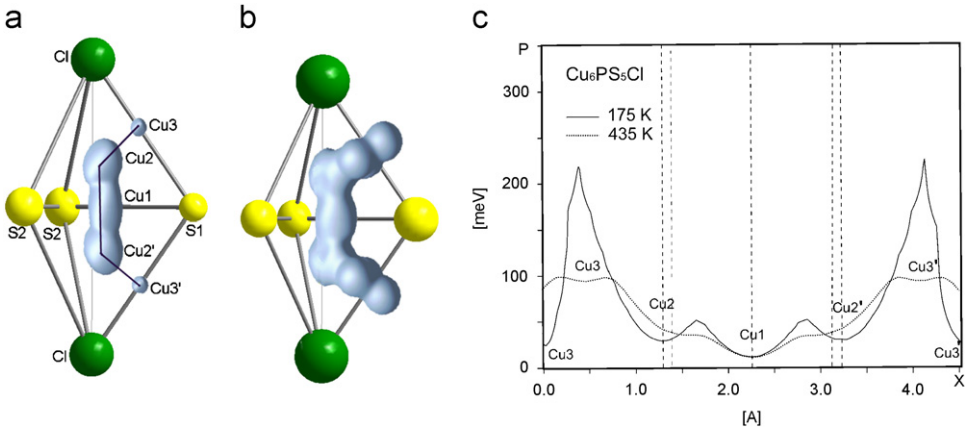

Fig. 5. Coordination of copper ions in superionic phase of Cu_6PS_5Cl at (a) 175 K and (b) 435 K, (c) pseudopotential within Cu3–Cu2–Cu1–Cu2–Cu3 diffusion path marked at (a).

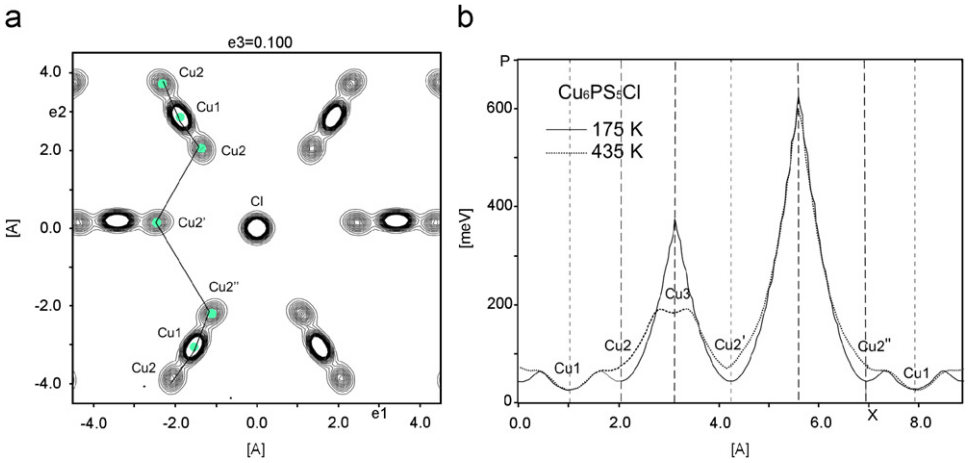

Fig. 7. (a) Joint PDFs of copper atoms with diffusion path, $T = 175\,K$, plane (111), (b) pseudopotentials along copper diffusion path.

positions. Fig. 7(a) presents the joint PDF of copper and chlorine atoms at 175 K as seen down the (111) direction, with the conduction path between copper clusters. On the basis of the joint PDF we calculated the pseudopotentials along the diffusion path at 175 and 435 K, see Fig. 7(b). With temperature increase the energy barrier between neighbouring copper Cu2′ and Cu2″ positions lowers only slightly from 0.58 eV at 175 K down to 0.53 eV at 435 K. Thus, similarly to Cu_6PS_5I, the hopping between these two positions must be facilitated by coupled oscillations of anion sublattice. From the other side it is probable that the role of Cu4 position in the conduction process is much more significant than it comes out from its weak electron density.

4. Conclusions

In the afford to explain the best conduction properties of Cu_6PS_5Cl among all Cu_6PS_5X's we performed X-ray single crystal study and domain structure observations. It has been proved that in the wide temperature range (down to $\approx 160\,K$) our crystals possess superionic properties connected with disordered cubic structure. Below $T_c = 160\,K$ ferroelastic transition to monoclinic *Cc* phase takes place. It is connected with ordering of copper substructure and as a consequence suppresses the copper motion. The temperature of this transition is strongly dependent on copper stoichiometry. On the other hand, the ordering process of copper ions starts at much higher temperatures on some impurities or crystal defects that results in precursor phenomena above T_c.

We determined copper diffusion paths on the basis of joint PDF of copper atoms in superionic phase and the potential barriers along diffusion paths.

Acknowledgments

We gratefully thank V.V. Panko for the crystal preparation and M. Polomska for the optical measurements.

This work was supported by the Polish State Committee for Scientific Research (project register 3 T08A 079 27).

Appendix A. Supplementary data

Supplementary data associated with this article can be found in the online version at 10.1016/j.jssc.2008.01.026.

References

[1] W.F. Kuhs, R. Nitsche, K. Scheunemann, Mat. Res. Bull. 14 (1979) 241.
[2] R.B. Beeken, J.J. Garbe, N.R. Petersen, J. Phys. Chem. Solids 64 (2003) 1261.
[3] A. Haznar, A. Pietraszko, I.P. Studenyak, Solid State Ionics 119 (1999) 31.
[4] A. Gagor, A. Pietraszko, D. Kaynts, J. Solid State Chem. 178 (2005) 3366.
[5] A. Gagor, A. Pietraszko, M. Drozd, M. Polomska, C. Pawlaczyk, D. Kaynts, J. Phys. Condens. Matter 18 (2006) 4489.
[6] S. Fiechter, E. Gmelin, Thermochim. Acta 87 (1985) 319.
[7] W.F. Kuhs, R. Nitsche, K. Scheunemann, Mat. Res. Bull. 11 (1976) 1115.
[8] I.P. Studenyak, M. Kranjcec, G.S. Kovacs, V.V. Panko, V.V. Mitrovcij, O.A. Mikajlo, Mater. Sci. Eng. B 97 (2003) 34.
[9] V. Petricek, M. Dusek, JANA2000, Institute of Physics, Praga, 2000.
[10] P. Coppens, X-ray Charge Densities and Chemical Bonding, Oxford University Press, Oxford, 1997.
[11] W.F. Kuhs, Acta Cryst. A 39 (1983) 148.
[12] R. Bachmann, H. Schulz, Acta Cryst. A 40 (1984) 668.
[13] W.L. Bond, Acta Cryst. 13 (1960) 814.
[14] D.I. Kaynts, I.P. Studenyak, I.I. Nebola, A.A. Horvat, Ukr. J. Phys. Opt. 3 (2002) 267.
[15] I.P. Studenyak, M. Kranjcec, G.S. Kovacs, V.V. Panko, Y.M. Azhniuk, I.D. Desnica, O.M. Bortes, Y.V. Voroshilov, Mater. Sci. Eng. B 52 (1998) 202.
[16] H. Aizu, J. Phys. Soc. Jpn. 27 (1968) 387.
[17] A. Gagor, Thesis, Wrocaw, 2007.
[18] T. Nilges, A. Pfitzner, Z. Kristallogr. 220 (2005) 281.
[19] J.K. Burdett, O. Eisenstain, Inorg. Chem. 31 (1992) 1758.
[20] A. Gagor, A. Pietraszko, D. Kaynts, V. Panko, Acta Cryst. A 62 (2006) 191.